

6. IN TIDE'S WAY: SOUTHEAST FLORIDA'S SEPTEMBER 2015 SUNNY-DAY FLOOD

WILLIAM V. SWEET, MELISA MENENDEZ, AYESHA GENZ, JAYANTHA OBEYSEKERA,
JOSEPH PARK, AND JOHN J. MARRA

The probability of a 0.57-m tidal flood within the Miami region has increased by >500% since 1994 from a 10.9-cm sea level rise (SLR)-related trend in monthly highest tides.

The Flood Event. High tides on 27 September 2015 flooded several Miami-region communities with 0.57 m of ocean water. The flooding was concerning because of the sunny-day conditions and awareness that trends of such events are accelerating within U.S. Atlantic Coast cities from rising seas (Sweet et al. 2014; Ezer and Atkinson 2014; Sweet and Marra 2016). It was the sixth largest flood measured by the National Oceanic and Atmospheric Administration (NOAA) tide gauge in Virginia Key, Florida (Miami region), since its 1994 installation (Fig. 6.1a). The five higher floods were in response to hurricanes.

The flood had substantial astronomical underpinnings (Fig. 6.1b); it occurred during spring tides and near the peak of the seasonal mean sea level (MSL), the lunar 8.8-year perigee, and the 18.6-year nodal cycles. These factors explain the 0.24-m NOAA tide prediction relative to mean higher high water (MHHW) tidal datum that delineates typical tidal inundation (Schureman 2001; Parker 2007). Yet, tide forcing alone was insufficient to produce the observed impacts as minor “nuisance” flooding begins in excess of 0.4 meters in this region (Sweet et al. 2014).

Other dynamics were at play. A nontidal sea level anomaly (Fig. 6.1b, green line), which exceeded 0.15 m for a month starting September 22, reached 0.33 m during the flood and even higher for weeks afterwards. Strong high pressure over Eastern Canada (Fig. 6.1c) with $>15 \text{ m s}^{-1}$ northeasterlies offshore of

the mid-Atlantic Bight (not shown) drove an Ekman-related setup along much of the U.S. East Coast. During the flood, setup was $>20 \text{ cm}$ along the southeast Florida coast as modeled by NOAA's extratropical surge and tide operational forecast system (Funakoshi et al. 2013). Local winds, however, were calm ($<3 \text{ m s}^{-1}$; <http://tidesandcurrents.noaa.gov/met>), inverse barometer effects nonexistent (Fig. 6.1c), and dynamical wave effects minimal as inferred by the $\sim 1 \text{ cm}$ standard deviations during tide measurements (Sweet et al. 2015). Interestingly, Gulf Stream transport measured upstream in the Florida Current (FC) slowed to a monthly minimum of 23.4 Sverdrup (Sv; $1 \text{ Sv} \equiv 10^6 \text{ m}^3 \text{ s}^{-1}$) on 25 September (Fig. 6.1d), which persisted through the flood. Transport slowdowns raise MSL along the US southeast (Zhao and Johns 2014; Ezer 2016) and Florida coasts (Park and Sweet 2015) from adjustments to meridional Ekman transport (Lee and Williams 1988) and shelf-wave dynamics (Czeschel et al. 2012; Ezer 2016). Previous studies report a 0.5–1.5 cm rise in coastal MSL per 1-Sv decline in Gulf Stream system transport (Ezer et al. 2013; Woodworth et al. 2014; Goddard et al. 2015; Ezer 2016); when it slows, local tidal-flood risks increase (Sweet et al. 2009; Ezer and Atkinson 2014; Wdowinski et al. 2016).

Here, we derive a contemporary return period of the flood using a time-dependent extreme value statistical model. Then, we assess the degree that (i) seasonal variability, (ii) tide cycles, (iii) FC monthly transport minimums, and (iv) a multidecadal trend have independently affected Virginia Key's extreme water level distribution and estimate their attribution during the flood. We conclude by analyzing how the flood's return period changes under future SLR projections for the Miami region forced by three representative concentration pathways (RCP).

Data and Methods. Verified 6-minute and monthly water levels, sampling standard deviations, and tide

AFFILIATIONS: SWEET—NOAA National Ocean Service, Silver Spring, Maryland; MENENDEZ—Environmental Hydraulic Institute, E.T.S., Universidad de Cantabria, Santander, Spain; GENZ—University of Hawaii, Honolulu, Hawaii; OBEYSEKERA—South Florida Water Management District, West Palm Beach, Florida; PARK—National Park Service, Everglades National Park, Homestead, Florida; MARRA—NOAA National Centers for Environmental Information, Honolulu, Hawaii.

DOI:10.1175/BAMS-D-16-0117.1

A supplement to this article is available online (10.1175/BAMS-D-16-0117.2)

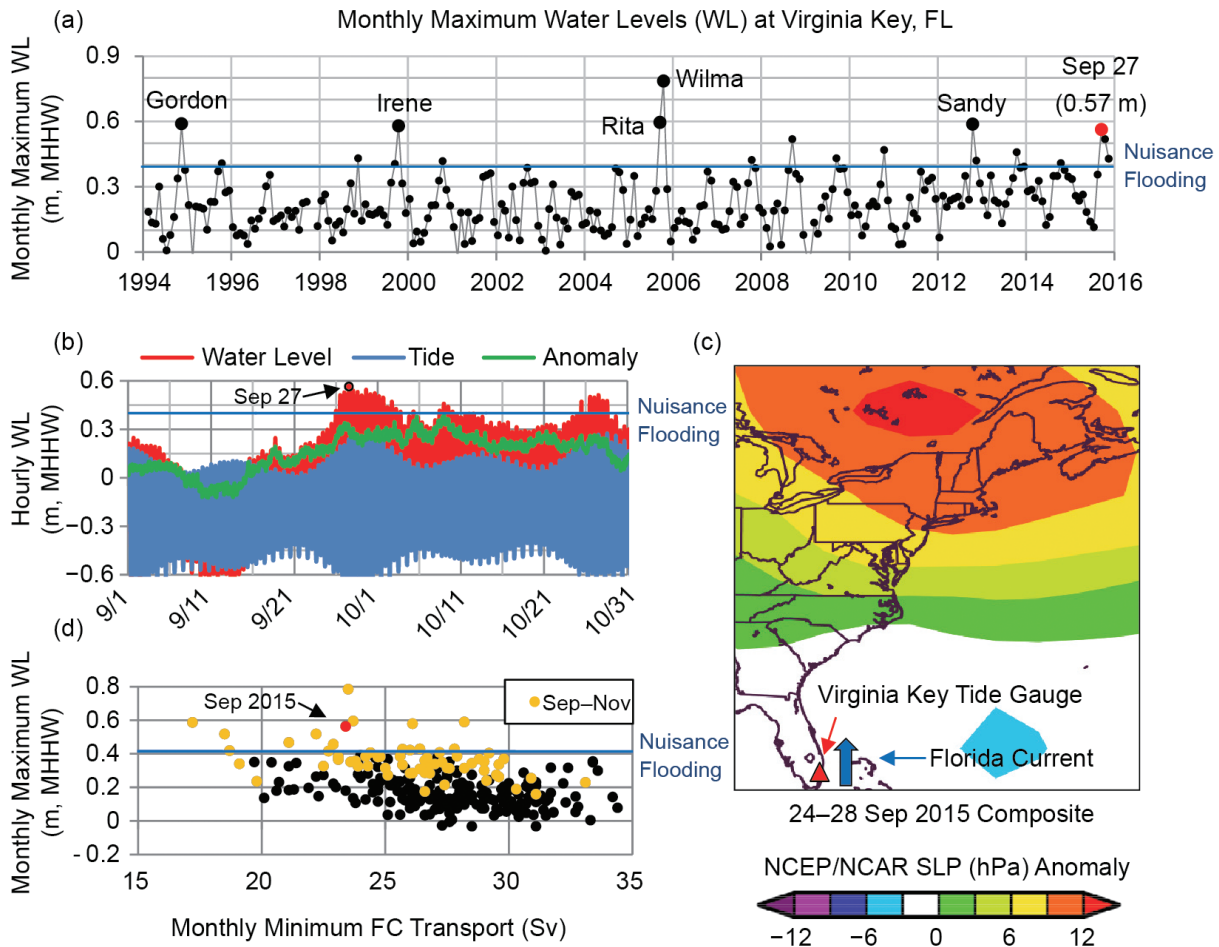


FIG. 6.1. (a) Highest monthly water levels (m) since 1994 at NOAA tide gauge Virginia Key, FL, indicating the local “nuisance” flood level; (b) hourly water levels (m) in Sep and Oct 2015 showing tidal and nontidal anomaly components highlighting the 27 Sep flood; (c) 5-day composite (www.esrl.noaa.gov/psd) of SLP (hPa) anomaly during the flood showing location of the tide gauge and FC measurements; and (d) scatterplot between monthly minimum FC transport (Sv) and monthly maximum water level (WL; m) highlighting Sep–Nov months (yellow) and the Sep 2015 event (red).

predictions are used for NOAA tide gauge Virginia Key (<http://tidesandcurrents.noaa.gov>). Daily FC transport is available from www.aoml.noaa.gov/phod/floridacurrent. We analyze monthly highest water levels using a generalized extreme value (GEV) model to assess flood height probabilities and decompose independent time-dependencies in the model’s location parameter. We follow methods of Menendez and Woodworth (2010) described in the online supplemental information.

Return level interval curves (Coles 2001) are constructed on a monthly and a 2015-annualized (12-month integrated) basis. Monthly return interval curves are vertically shifted by the time-dependent location parameter components (equation 2 in the online supplemental information) to assess climate

variability and trend effects on the flood’s return period. We use the classic (annual scale) curves to compute future projections for annual relevancy purposes. Return periods are approximated as $-1/\ln(F_z)$, where F is the cumulative probability of a flood with height z , instead of the traditional $1/(1-F_z)$ method (Beran and Nozdryn-Plotnicki 1977; Coles 2001) to better estimate shorter return periods (e.g., <1 year).

What role did climatic variability and trends play in the September 2015 flood? Our model estimates that a 0.57-m flood has a 6-year return period (black curve in Fig. 6.2a) during Septembers assuming conditions (e.g., nodal cycle, FC transport) match those during September 2015. The flood has a 3-year return period when considering (integrating across) all months

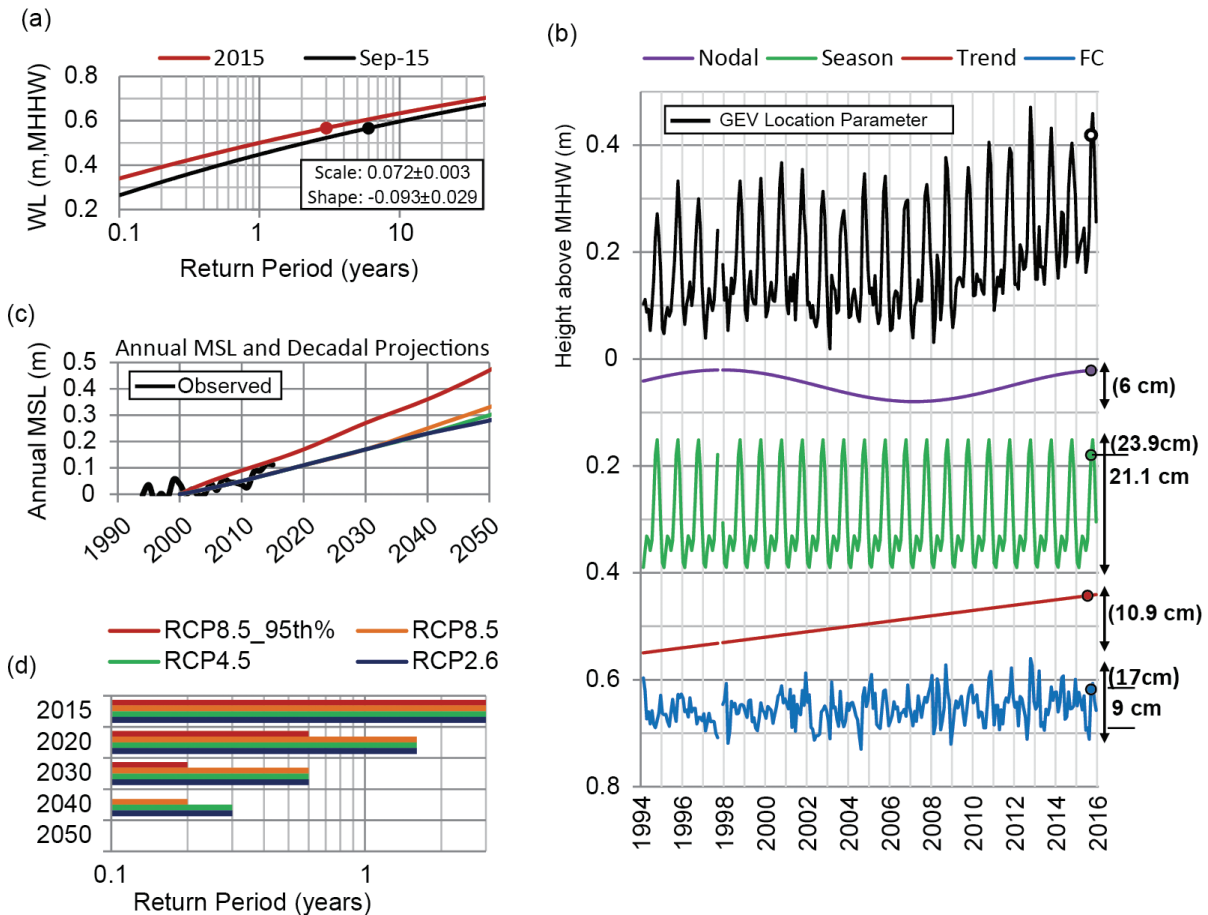


FIG. 6.2. (a) GEV-estimated return level interval curves from monthly maximum WL (m) at Virginia Key for Sep 2015 (black curve) and annualized for all months in 2015 (red curve) indicating the 27 Sep flood level (dots) and GEV model parameter standard errors. (b) Time-varying location parameter (black line) and its components (plotted to scale but with arbitrary values) with component magnitudes (m) during the 27 Sep flood (circles) and their total ranges in parenthesis. (c) Annual MSL (m) at Virginia Key since 1994 overlaid upon local RCP-based SLR projections of Kopp et al. (2014). (d) Return periods by decade of the Sep 2015 flood height (0.57 m above MHHW) in response to SLR projections.

during 2015 (red curve in Fig. 6.2a), reflecting the peak seasonal location parameter during Octobers (Fig. 6.2b, green line). Highest water levels occur September–November (Fig. 6.1d, yellow dots), typically during Octobers. If a 0.57-m flood occurred in February 2015 when the seasonal location parameter is minimum (21.1 cm lower than in September), a higher (less probable) water level would be required; it would have a >100-year return period. Our estimates (Fig. 6. 2a) are based upon a 22-year data record with a sample size 7 times longer than the flood’s annualized return period, which results in low GEV-parameter estimate uncertainties (Fig. 6.2a). We note our return periods agree with those from a 50-year record from the nearby historic Miami NOAA gauge (<http://tidesandcurrents.noaa.gov/est>; Zervas 2013) and our

seasonal location-parameter range of 23.9 cm matches its 23.7-cm MSL cycle (Zervas 2009).

The 18.6-year lunar nodal cycle is estimated as having a 6-cm location-parameter range, which was near-peak during the flood (Fig. 6.2b). If at its minimum (and all other factors the same), the return period of this flood occurring in a September would have been 16.5 years instead of 6 years (>150% probability increase). The periodicity of the lunar perigee, which amplifies the tidal range on a ~4.4-year cycle (Haigh et al. 2011), was included in our model but found to be insignificant. Similarly, had the flood occurred during a September with higher FC transport (e.g., 33.1 Sv in September 1997 and a 9-cm location parameter decrease shown in Fig. 6.2b), the return period would have been 29 years instead

of 6 years (>350% probability increase). Our model estimates a 17-cm total range in location parameter due to co-variability with FC transport minimums, equating to a 0.9 ± 0.2 cm increase for every 1-Sv decline, which agrees with previous estimates. Lastly, our model estimates a long-term trend in the location parameter of 0.5 ± 0.1 cm year⁻¹ (10.9 cm rise since beginning of 1994), which closely matches the trend in MSL (~11 cm in Fig. 6.2c). If the flood had occurred in September 1994, its return period would have been 39 years instead of 6 years (>500% probability increase).

What does the future hold in terms of more September 2015 flooding? The logical question is *how much more frequent will these kinds of floods become in the future?* To answer this question, the September 2015 flood is assessed in terms of its annualized return period (3 years; red curve in Fig. 6.2a), although flood frequencies will likely remain most prevalent during the fall (e.g., Fig. 6.1d). It is assumed that future changes in tidal flooding will occur only in response to local SLR, though variability (shown here) is significant. We use the 50th and 95th% SLR projections for Virginia Key forced by RCPs modeled by Kopp et al. (2014), which correspond to global SLR of 0.5–1.21 m by 2100. An overlay of Virginia Key’s annual MSL (Fig. 6.2c) shows a current trajectory between the 50th and 95th% of the RCP 8.5 SLR projections. By 2030, the flood is likely to become a 0.6-year event (~twice a year) under the median RCP 2.6, 4.5, and 8.5 projections (Fig. 6.2d) and a 0.2-year event (≥ 5 times a year) under the 95th% of the RCP 8.5 projection. With 0.2 m more local SLR, which is exceeded under all local SLR projections between 2040–2050, the flood will occur >10 times a year (<0.1 year return period).

Conclusion. Our time-dependent GEV model disentangles and probabilistically decomposes independent contributions from concurrent processes attributing to the Miami-region floods during 27 September 2015. Seasonal and tide cycles are quite predictable, whereas FC transport variability is less so (e.g., DiNezio et al. 2009). In terms of decades-old infrastructure, two major factors were at play: a 9-cm increase from FC variability and a 10.9-cm rise from a climate-related SLR trend since 1994 of which a fraction (~0.05 cm year⁻¹) is downward vertical land motion (Zervas et al. 2013; Kopp et al. 2014) common to south Florida. There is a decreasing trend (significant at the 99% level) in monthly minimum FC transport of 2.3 Sv since 1994, which likely

contributed ~2 cm to the SLR-related trend (Fig. 6.2b, blue line).

A decline in the large-scale Gulf Stream transport, which is expected this century (Yin 2012) to exacerbate flooding along the mid-Atlantic (Hall et al. 2016), is not well resolved for the FC locally within the SLR projections (Kopp et al. 2014). Because of this, and since we use a parametric extreme distribution to quantify the transition to a more recurrent event better estimated empirically (Sweet and Park 2014), our flood-frequency projections should be considered conservative underestimates. In closing, flooding on 27 September inundated 0.57 m of normally dry land (~2 feet; <https://coast.noaa.gov/slr>) and capped a week-long event in which daily high tides exceeded the local nuisance flood threshold (Fig. 6.1b). Tidal floods of this magnitude occur only every few years now but will become commonplace in the coming decades.

ACKNOWLEDGEMENTS. The authors thank NOAA for hosting and providing public access to their ocean and atmospheric data, without which, this work would not be possible. Melisa Menendez’s contribution was made possible through the Spanish Ramon y Cajal program (RYC-2014-16469)

REFERENCES

- Beran, M. A., and M. K. Nozdryn-Plotnicki, 1977: Estimation of low return period floods. *Hydrol. Sci. Bull.*, **2**, 275–282, doi:10.1080/02626667709491717.
- Coles, S., 2001: *An Introduction to Statistical Modeling of Extreme Values*. Springer, 208 pp.
- Czeschel, L., C. Eden, and R. J. Greatbatch, 2012: On the driving mechanism of the annual cycle of the Florida current transport. *J. Phys. Oceanogr.*, **42**, 824–839, doi:10.1175/JPO-D-11-0109.1.
- DiNezio, P. N., L. J. Gramer, W. E. Johns, C. S. Meinen, and M. O. Baringer, 2009: Observed interannual variability of the Florida Current: wind forcing and the North Atlantic Oscillation. *J. Phys. Oceanogr.*, **39**, 721–736, doi: 10.1175/2008JPO4001.1.
- Ezer, T., 2016: Can the Gulf Stream induce coherent short-term fluctuations in sea level along the U.S. East Coast?: A modeling study. *Ocean Dyn.*, **66**, 207–220, doi:10.1007/s10236-016-0928-0.
- , and L. P. Atkinson, 2014: Accelerated flooding along the U.S. East Coast: On the impact of sea level rise, tides, storms, the Gulf Stream and NAO. *Earth’s Future*, **2**, 362–382, doi:10.1002/2014EF000252.

- , —, W. B. Corlett, and J. L. Blanco, 2013: Gulf Stream's induced sea level rise and variability along the U.S. mid-Atlantic coast. *J. Geophys. Res. Oceans*, **118**, 685–697, doi:10.1002/jgrc.20091.
- Funakoshi, Y., J. C. Feyen, F. Aikman III, A. van der Westhuysen, and H. Tolman, 2013: The Extratropical Surge and Tide Operational Forecast System (ESTOFS) Atlantic Implementation and Skill Assessment. NOAA Tech. Rep. NOS CS 32, 147 pp. [Available online at www.nauticalcharts.noaa.gov/csdl/publications/TR_NOS-CS32-FY14_01_Yuji_ESTOFS_SKILL_ASSESSMENT.pdf.]
- Goddard, P. B., J. Yin, S. M. Griffies, and S. Zhang, 2015: An extreme event of sea-level rise along the Northeast coast of North America in 2009–2010. *Nature Comm.*, **6**, 6346, doi:10.1038/ncomms7346.
- Haigh, I. D., M. Eliot, and C. Pattiaratchi, 2011: Global influences of the 18.61 year nodal cycle and 8.85 year cycle of lunar perigee on high tidal levels. *J. Geophys. Res.*, **116**, C06025, doi:10.1029/2010JC006645.
- Hall, J. A., S. Gill, J. Obeysekera, W. Sweet, K. Knuuti, and J. Marburger, 2016: Regional sea level scenarios for coastal risk management: Managing the uncertainty of future sea level change and extreme water levels for Department of Defense coastal sites worldwide. U.S. Department of Defense, Strategic Environmental Research and Development Program, 224 pp. [Available online at www.usfsp.edu/icar/files/2015/08/CARSWG-SLR-FINAL-April-2016.pdf.]
- Kopp, R. W., R. M. Horton, C. M. Little, J. X. Mitrovica, M. Oppenheimer, D. J. Rasmussen, B. H. Strauss, and C. Tebaldi, 2014: Probabilistic 21st and 22nd century sea-level projections at a global network of tide gauge sites. *Earth's Future*, **2**, 383–406, doi:10.1111/ef2.2014EF000239.
- Lee, T. N., and E. Williams, 1988: Wind-forced transport fluctuations of the Florida Current. *J. Phys. Oceanogr.*, **18**, 937–946.
- Menéndez, M., and P. L. Woodworth, 2010: Changes in extreme high water levels based on a quasi-global tide-gauge data set. *J. Geophys. Res.*, **115**, C10011, doi:10.1175/2011JCLI3932.1.
- Park, J., and W. Sweet, 2015: Accelerated sea level rise and Florida current transport. *Ocean Sci.* **11**, 607–615, doi:10.5194/os-11-607-2015.
- Parker, B. B., 2007: Tidal analysis and prediction. NOAA Special Report NOS CO-OPS 3, 378 pp. [Available online at www.co-ops.nos.noaa.gov/publications/Tidal_Analysis_and_Predictions.pdf.]
- Schureman, P., 2001: Manual of harmonic analysis and prediction and tides. Special Publication 98, U.S. Department of Commerce Coast and Geodetic Survey, 317 pp.
- Sweet, W. V. and J. Park, 2014: From the extreme to the mean: Acceleration and tipping points of coastal inundation from sea level rise. *Earth's Future*, **2**, 579–600, doi:10.1002/2014EF000272.
- , and J. J. Marra, 2016: 2015 State of U.S. “nuisance” tidal flooding. Supplement to *State of the Climate: National Overview* for May 2016. [Available online at www.ncdc.noaa.gov/monitoring-content/sotc/national/2016/may/sweet-marra-nuisance-flooding-2015.pdf.]
- , C. Zervas, and S. Gill, 2009: Elevated East Coast sea level anomaly: June–July 2009. NOAA Tech. Rep. NOS CO-OPS 051, 30 pp. [Available online at http://tidesandcurrents.noaa.gov/publications/EastCoast-SeaLevelAnomaly_2009.pdf.]
- , J. Park, J. J. Marra, C. Zervas, and S. Gill, 2014: Sea level rise and nuisance flood frequency changes around the United States. NOAA Tech. Rep. NOS CO-OPS 73, 53 pp. [Available online at http://tidesandcurrents.noaa.gov/publications/NOAA_Technical_Report_NOS_COOPS_073.pdf.]
- , —, S. Gill, and J. Marra, 2015: New ways to measure waves and their effects at NOAA tide gauges: A Hawaiian-network perspective. *Geophys. Res. Lett.*, **42**, doi:10.1002/2015GL066030.
- Wdowinski, S., B. Ronald, B. P. Kirtman, and Z. Wu, 2016: Increasing flooding hazard in coastal communities due to rising sea level: Case study of Miami Beach, Florida. *Ocean Coastal Manage.*, **126**, 1–8, doi:10.1016/j.ocecoaman.2016.03.002.
- Woodworth, P. L., M. Maqueda, M. Á. Roussenov, V. M. Williams, and R. G. Hughes, 2014: Mean sea level variability along the northeast American Atlantic coast, and the roles of the wind and the overturning circulation. *J. Geophys. Res. Oceans*, **119**, 8916–8935, doi:10.1002/2014JC010520.
- Yin, J., 2012: Century to multi-century sea level rise projections from CMIP5 models. *Geophys. Res. Lett.*, **39**, L17709, doi:10.1029/2012GL052947.
- Zervas, C., 2009: Sea level variations of the United States 1854–2006. NOAA Tech. Rep. NOS CO-OPS 053, Appendices I–V. [Available online at http://tidesandcurrents.noaa.gov/publications/Tech_rpt_53.pdf.]

- , 2013: Extreme water levels of the United States 1893–2010. NOAA Tech. Rep. NOS CO-OPS 67, Appendices I–VIII. [Available online at http://tidesandcurrents.noaa.gov/publications/NOAA_Technical_Report_NOS_COOPS_067a.pdf.]
- Zervas, C., S. Gill, and W. V. Sweet, 2013: Estimating vertical land motion from long-term tide gauge records. Tech. Rep. NOS CO-OPS 65, 22 pp. [Available online at http://tidesandcurrents.noaa.gov/publications/Technical_Report_NOS_CO-OPS_065.pdf.]
- Zhao, J., and W. Johns, 2014: Wind-forced interannual variability of the Atlantic Meridional Overturning Circulation at 26.5°N. *J. Geophys. Res. Oceans*, **119**, 2403–2419, doi:10.1002/2013JC009407.